

## Magnetic transition and orbital degrees of freedom in vanadium spinels

Hirokazu Tsunetsugu

*Yukawa Institute for Theoretical Physics, Kyoto University, Kyoto 606-8502, Japan*

Yukitoshi Motome\*

*Tokura Spin Superstructure Project, ERATO, Japan Science and Technology Corporation, c/o National Institute of Advanced Industrial Science and Technology Tsukuba Central 4, Tsukuba, Japan*

(Received 30 April 2003; published 27 August 2003)

We propose a scenario for the two phase transitions in  $AV_2O_4$  ( $A = \text{Zn, Mg, Cd}$ ), based on an effective spin-orbital model on the pyrochlore lattice. At high temperatures, spin correlations are strongly frustrated due to the lattice structure, and the transition observed at  $\sim 50$  K is attributed to an orbital order, supported by Jahn-Teller lattice distortion. This orbital order introduces spatial modulation of spin-exchange couplings depending on the bond direction. This partially releases the frustration and leads to a spin order observed at  $\sim 40$  K. We also study the stable spin configuration by taking account of third-neighbor exchange couplings and quantum fluctuations. The result is consistent with the experimental results.

DOI: 10.1103/PhysRevB.68.060405

PACS number(s): 75.10.Jm, 75.30.Et, 75.30.Ds, 75.50.Ee

Pyrochlore lattice is a network of corner-sharing tetrahedra shown in Fig. 1, and it is a typical geometrically frustrated system in three dimensions. The vanadium spinel  $\text{ZnV}_2\text{O}_4$  is an insulator, and its sublattice of magnetic vanadium ions constitutes a pyrochlore lattice. It was found that this compound reveals two phase transitions at  $T_{c1} = 50$  K and  $T_{c2} = 40$  K.<sup>1</sup> An x-ray-diffraction experiment showed that the transition at  $T_{c1}$  is a structural transition from the high-temperature cubic phase to the low-temperature tetragonal phase with the lattice constants  $a = b > c$ . The neutron experiment at  $T = 4.2$  K showed the presence of the antiferromagnetic long-range order plotted in Fig. 1,<sup>2</sup> and the Li-substitute material showed an anomaly in its nuclear magnetic resonance (NMR) signal at  $T_{c2}$ .<sup>1</sup> These indicate that the lower-temperature transition in  $\text{ZnV}_2\text{O}_4$  is a paramagnetic-to-antiferromagnetic transition.

Theoretical studies have predicted unusual properties for spin systems on the pyrochlore lattice. In particular, antiferromagnetic classical spin systems with only nearest-neighbor interactions are believed to have no magnetic order at any temperature.<sup>3-5</sup> It is also believed that the quantum-spin systems have a spin-singlet ground state and a finite energy gap to spin-triplet excitations with thermodynamic number of singlet states inside the singlet-to-triplet gap.<sup>6</sup> Several symmetry breakings are theoretically predicted within the spin singlet subspace, e.g., dimer/tetramer order, but without magnetic long-range order.<sup>7-10</sup>

Therefore, we encounter a difficulty in explaining these phase transitions in  $\text{ZnV}_2\text{O}_4$ , if the material is considered as a pure spin  $S = 1$  system on the pyrochlore lattice and other degrees of freedom are necessary to take into account. Yamashita and Ueda studied this problem based on a valence-bond-solid (VBS) approach and examined the effects of Jahn-Teller distortion.<sup>11</sup> They proposed that the transition at  $T_{c1}$  is due to the Jahn-Teller effect which lifts the degeneracy of the spin-singlet local ground states at each tetrahedron unit of the pyrochlore lattice. This idea was also applied to classical spin systems, and the effects of the coupling to the lattice distortion were investigated using the point-group ar-

gument and the Landau theory.<sup>12</sup> These scenarios are quite appealing, but some difficulty still seems to remain.

The problem is that it is difficult to explain the magnetic order below the low transition temperature  $T_{c2}$  by Yamashita-Ueda-type scenarios based on a quantum-spin picture. Like other theoretical works, they started from the assumption that there exists a finite energy gap between the spin-singlet ground state and spin-triplet excitations, and constructed a low-energy effective theory to describe a phase transition within the spin-singlet sector. High-energy excitations with total spin  $S \neq 0$  are already traced out from the theoretical framework, and there remain no degrees of freedom describing the low-temperature magnetic transition.

Scenarios based on a classical spin picture do not have this problem, but it has another difficulty to explain the following generic difference between the vanadium and chromium spinels. The presence of these two transitions is common to other vanadium spinels,  $\text{MgV}_2\text{O}_4$  (Ref. 13) and  $\text{CdV}_2\text{O}_4$ ,<sup>14</sup> with the same valence  $V^{3+}$ . On the other hand, the chromium spinels  $\text{ZnCr}_2\text{O}_4$ ,  $\text{CdCr}_2\text{O}_4$ , and  $\text{MgCr}_2\text{O}_4$

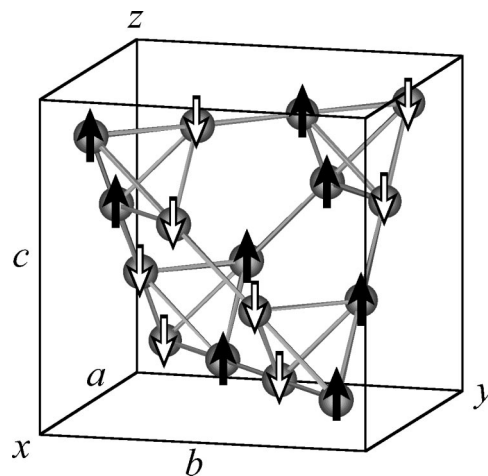


FIG. 1. Cubic unit cell of the pyrochlore lattice and spin order determined by neutron experiments at low temperatures.

show only one transition at 12.5 K, 7.8 K, and 12.5 K, respectively.<sup>15,16</sup> The difference between the vanadium spinels and the chromium spinels is generic and independent of divalent *A*-site cations. It is also unclear whether classical approximations are justified at low temperatures for the system with the second smallest spin,  $S=1$ .

In the present study, we will explore another scenario to explain the two transitions with taking account of the orbital degrees of freedom, which exist in the vanadium spinels but not in the chromium spinels. The essential difference between the vanadium and chromium spinels is the number of electrons in magnetic ions:  $V^{3+}$  ions has  $d^2$  configuration and  $Cr^{3+}$  has  $d^3$  configuration. Due to the cubic crystal field, the  $d$ -electron orbitals are split into the high-energy  $e_g$  and low-energy  $t_{2g}$  multiplets. Since in both the spinels the high spin state is realized due to large intra-atomic Coulomb interactions, two of the threefold degenerate  $t_{2g}$  orbitals are occupied by electrons in the vanadium case, whereas all three orbitals are occupied in the chromium case. Therefore, each  $V^{3+}$  ion has threefold orbital degeneracy in addition to the triplet spin state  $S=1$ . Rigorously speaking, the crystal field has a small trigonal component, which may result in a further splitting of the  $t_{2g}$  multiplet. However, this splitting is compensated by the covalency difference of the three states, and the net splitting will be small and we neglect this.

The realistic model Hamiltonian for this system reads with the standard notation,

$$H = \sum_{\langle i,j \rangle} \sum_{\alpha\beta} \sum_{\sigma} [t_{\alpha\beta}(\mathbf{r}_i - \mathbf{r}_j) c_{i\alpha\sigma}^\dagger c_{j\beta\sigma} + \text{H.c.}] + \frac{1}{2} \sum_i \sum_{\alpha\beta, \alpha'\beta'} \sum_{\sigma\tau} U_{\alpha\beta, \alpha'\beta'} c_{i\alpha\sigma}^\dagger c_{i\beta\tau}^\dagger c_{i\beta'\tau} c_{i\alpha'\sigma}, \quad (1)$$

where  $i, j$  are site indices,  $\sigma, \tau$  are spin indices, and  $\alpha, \beta = 1$  ( $d_{yz}$ ), 2 ( $d_{zx}$ ), 3 ( $d_{xy}$ ) are orbital indices. For the Coulomb interactions, we use the standard parametrization,  $U_{\alpha\beta, \alpha'\beta'} = V\delta_{\alpha\alpha'}\delta_{\beta\beta'} + J(\delta_{\alpha\beta'}\delta_{\beta\alpha'} + \delta_{\alpha\beta}\delta_{\alpha'\beta'})$ , and  $U = V + 2J$  is the Hubbard interaction in the same orbital. These values were determined from the spectroscopy data for the vanadium perovskites as  $U \sim 6$  eV and  $J \sim 0.7$  eV,<sup>17</sup> and it is reasonable to assume a small value for the ratio of the two in the vanadium spinels,  $\eta \equiv J/U \sim 0.11$ . The hopping integrals  $t_{\alpha\beta}(\mathbf{r}_i - \mathbf{r}_j)$  were also determined by a parameter fitting of the first-principle band calculation data,<sup>18</sup> and it was found that the one for the nearest-neighbor  $\sigma$  bond is much larger than the others. We therefore consider only this kind of hoppings,  $t_\sigma = -0.32$  eV, and set the others zero. This is the hopping in the case where one of four lobes of each  $t_{2g}$  orbital is pointing towards the other end of the bond. In this case, the number of electrons in each orbital is conserved through the hopping processes, simplifying the following calculations. We neglect the relativistic spin-orbit coupling, which is much smaller than the energy scales in Eq. (1).

Since  $ZnV_2O_4$  is an insulator, we employ the strong coupling approach,  $U \gg |t_\sigma|$ , and include the hopping processes

by the second-order perturbation.<sup>19</sup> Each vanadium ion  $V^{3+}$  has  $d^2$  configuration and it is in a high spin state,  $S=1$ , due to large intra-atomic interactions. Each vanadium site is represented by a spin state  $S_i^z = 0, \pm 1$  and an orbital configuration  $\{n_{i\alpha}\}_{\alpha=1}^3$ , which is subject to the local constraint,  $\sum_\alpha n_{i\alpha} = 2$ , imposed by the valence of the vanadium ion. Different local states are hybridized by the hopping processes, and this is described by an effective spin-orbital (so) model of Kugel-Khomskii type on the pyrochlore lattice. It reads

$$H_{\text{so}} = \sum_{\langle i,j \rangle} [H_{\text{o-AF}}^{(ij)} + H_{\text{o-F}}^{(ij)}], \quad (2)$$

$$H_{\text{o-AF}}^{(ij)} = -K_0(A + B\mathbf{S}_i \cdot \mathbf{S}_j)[n_{i\alpha(ij)}(1 - n_{j\alpha(ij)}) + (1 - n_{i\alpha(ij)})n_{j\alpha(ij)}], \quad (3)$$

$$H_{\text{o-F}}^{(ij)} = -K_0C(1 - \mathbf{S}_i \cdot \mathbf{S}_j)n_{i\alpha(ij)}n_{j\alpha(ij)}, \quad (4)$$

where  $K_0 = t_\sigma^2/U > 0$ ,  $A = (1 - \frac{2}{3}\eta)/(1 - 2\eta)$ ,  $B = \frac{2}{3}\eta/(1 - 2\eta)$ ,  $C = (1 + \eta)/(1 + 2\eta)$ , and  $\eta = J/U$  as defined before.  $\alpha(ij)$  denotes the orbital in which electron hopping is possible between the sites  $i$  and  $j$ .

The two parts  $H_{\text{o-AF}}^{(ij)}$  and  $H_{\text{o-F}}^{(ij)}$  represent the orbital ‘‘antiferro’’ and ‘‘ferro’’ interactions, respectively. The sign of the spin-exchange term in these two indicates that an antiferro-orbital configuration favors a ferromagnetic spin state, while a ferro-orbital configuration favors an antiferromagnetic one, as is usual for the Kugel-Khomskii effective model. It is noted that the orbital parts contain only density-density interactions as a consequence of the above-mentioned character of the hopping integrals. This means that the orbital interaction has a large anisotropy and the anisotropy axis depends on the bond direction of two neighboring sites, in contrast to the spin space with full rotational symmetry.

We now give a simple argument to discuss the character of orbital and spin fluctuations at high temperatures where no symmetry breaking takes place. To discuss spin fluctuations, we replace orbital density operators by their mean value,  $n_{i\alpha} \rightarrow \langle n_{i\alpha} \rangle = \frac{2}{3}$ , and the result is a simple Heisenberg model on the pyrochlore lattice with the nearest-neighbor coupling  $J_s = \frac{4}{9}K_0(C - B)$  which is antiferromagnetic for the realistic value of  $\eta \sim 0.11$ . This is a strongly frustrated system and the enhancement of spin correlations with decreasing temperature will be quite small. The situation in the orbital part is different due to its anisotropy. This time, we replace the spin operators by their mean value,  $\mathbf{S}_i \rightarrow \langle \mathbf{S}_i \rangle = \mathbf{0}$ , and obtain the following effective orbital Hamiltonian:

$$H_{\text{orb}} = K_0 \sum_{\langle i,j \rangle} [(2A - C)n_{i\alpha(ij)}n_{j\alpha(ij)} - A(n_{i\alpha(ij)} + n_{j\alpha(ij)})], \quad (5)$$

but the linear terms in  $n_{i\alpha}$  become a constant after taking the summation over bonds because of the local constraint. Since  $2A - C \sim 1$  for small  $\eta$ , the orbital interactions are ‘‘antiferromagnetic,’’ but the number of local orbital states is 3 not 2, which corresponds to a three-state Potts model (or equiva-

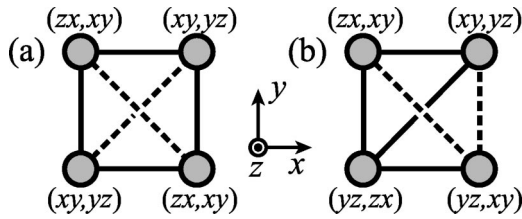


FIG. 2. Mean-field ground states of the effective orbital model (5). Configuration in a tetrahedron unit cell is shown. Labels  $xy$ , etc., indicate two occupied orbitals at each site. Solid (dash) lines denote antiferro-orbital (ferro-orbital) bonds, which have ferromagnetic (antiferromagnetic) spin couplings.

lently a three-state clock model). More importantly, the anisotropy axis varies from bond to bond depending on its direction.

We now consider the stable orbital configuration of  $H_{\text{orb}}$ . As for a tetrahedron unit, there are essentially two different types of stable configurations shown in Fig. 2. In the first type [Fig. 2(a)], two ferro-orbital bonds do not touch each other, while they touch at one site in the second type [Fig. 2(b)], and these two types have the same energy,  $-(4A + 2C)K_0$ . Apart from the examples shown in Fig. 2, there are 2 and 3 other equivalent configurations belonging to the first and second type, respectively.

The degeneracy in energy between the two types of configurations is lifted if the Jahn-Teller coupling is taken into account. Below the higher transition temperature  $T_{c1}$ , the system is compressed along the  $c$  axis. Considering the corresponding shift of oxygen atoms along the  $c$  axis, the energy level of  $d_{xy}$  orbital is pushed down relative to the other orbitals, and we write the level separation as  $\Delta_{JT}$ . The energy correction is then  $-\frac{4}{3}\Delta_{JT}$  and  $-\frac{1}{3}\Delta_{JT}$  for the two orbital configurations shown in Figs. 2(a) and 2(b), respectively. The energy difference is due to the difference in the number of occupied  $d_{xy}$  orbitals. Therefore, it is natural to understand that the higher-temperature transition is an orbital ordering of the type in Fig. 2(a).

This orbital order introduces a spatial modulation of spin-exchange couplings and leads to the reduction of the spin frustration as a consequence. As seen from Eqs. (2)–(4), a ferro-orbital bond has an antiferromagnetic spin coupling ( $J_{1A} = K_0C$ ), while an antiferro-orbital bond has a ferromagnetic coupling ( $J_{1F} = -K_0B$ ). The spatial pattern of spin exchange couplings is shown in Fig. 3(a). Since the antiferromagnetic couplings are much stronger than the ferromagnetic ones,  $J_{1A} \gg |J_{1F}|$  for the realistic value of  $\eta$ , antiferromagnetic spin alignment is stabilized in each chain in the  $xy$  planes, and the entire spin configuration will be built up by stacking of antiferromagnetic chains.

Interactions between the antiferromagnetic chains are ferromagnetic ones,  $J_{1F}$ , but frustrated as shown in Fig. 3(a). The frustration is due to the structure of the pyrochlore lattice and also antiferromagnetic spin correlations in each chain, but the sign of interchain couplings  $J_{1F}$  is not essential. Therefore, the relative angle of spins between different chains remains undetermined in the mean-field level approximation for the spin-orbital model  $H_{\text{so}}$ , and it is determined by some other mechanisms.

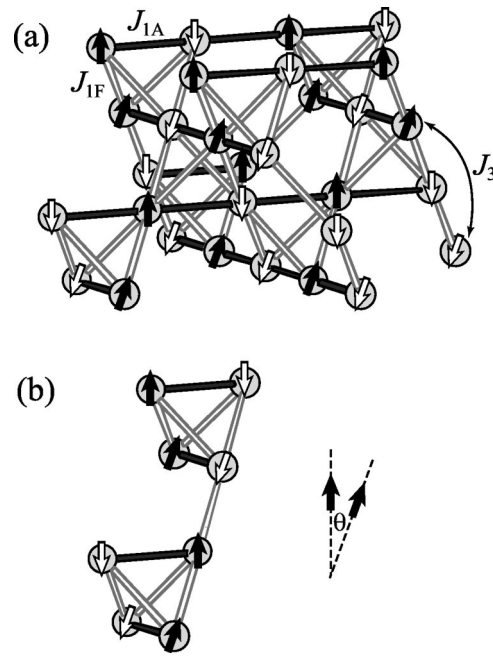


FIG. 3. (a) Spin-exchange couplings in the orbital ordered state. Strong antiferromagnetic couplings and weak ferromagnetic couplings are shown by black and white bonds, respectively.  $J_3$  is the third-neighbor interaction. (b) Magnetic unit cell of the  $\mathbf{q} = (0,0,2\pi/c)$  state.

The first mechanism to consider is longer-range exchange interactions, in particular, the third neighbor interactions ( $J_3$ ). Fitting of the band calculation results predicted that the  $\sigma$  bond of third-neighbor pairs has a larger amplitude than for second-neighbor pairs,<sup>18</sup> and, more importantly, exchange couplings are frustrated between second-neighbor pairs. The third-neighbor exchange coupling has a large amplitude and it is also antiferromagnetic. Therefore, this implies an order with  $\mathbf{q} = (0,0,2\pi/c)$ . Two tetrahedron unit cells in two neighboring  $xy$  planes have spin configurations opposite to each other. However, the relative angle  $\theta$  between the spins in the bottom plane of each tetrahedron and those for the top plane is not yet determined.

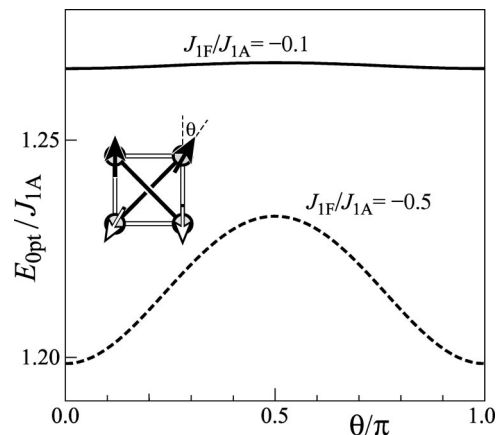


FIG. 4. Zero-point energy of quantum fluctuations as a function of  $\theta$ , the angle of local staggered moments between the neighboring chains.

The second mechanism is fluctuations of spins, and we here determine the relative angle  $\theta$  which minimizes the zero-point energy of quantum fluctuations.<sup>20</sup> We use the standard spin wave approach starting with the magnetic unit cell containing eight sites as shown in Fig. 3(b). By means of the Bogoliubov transformation, the energy dispersion of magnons is calculated,  $\omega_{\mathbf{k}\gamma}$ , where  $\gamma$  labels the magnon branch, and the zero-point energy is obtained by  $E_{0\text{pt}}(\theta) = \Omega^{-1} \sum_{\mathbf{k}\gamma} \omega_{\mathbf{k}\gamma}$ , where  $\Omega$  is the number of sites and  $\hbar = 1$  in our units. Calculations have been performed for various values of  $J_{1F}/J_{1A}$  and typical results are shown in Fig. 4. Here we set  $J_3 = 0$  for simplicity, since this term is not essential for determining  $\theta$ . The zero-point energy is always minimum at  $\theta = 0, \pi$ , which means that collinear order is the stablest, and these two are equivalent since they are related to each other by the mirror symmetry with respect to the  $x = y$  plane. This spin order agrees with the experimental result shown in Fig. 1. The transition temperature  $T_{c2} \sim 40$  K provides an order estimate of the third-neighbor exchange interaction  $J_3$  and also of the stabilization energy due to quantum fluctuations. However, a more quantitative estimate needs an analysis beyond the scope of this paper and this is a problem for future study.

In this paper, we have proposed a scenario for the two phase transitions in the vanadium spinels  $AV_2O_4$  ( $A = \text{Zn},$

$\text{Mg}, \text{Cd}$ ). In our scenario, the high-temperature transition observed at  $\sim 50$  K is an orbital order assisted by the Jahn-Teller distortion. This orbital order introduces spatial modulation of spin-exchange couplings. The geometrical spin frustration is consequently relaxed, and this induces the low-temperature magnetic transition experimentally observed at  $\sim 40$  K. If there is no orbital order, the system remains subject to strong frustration, and we believe that this is the case for  $\text{ACr}_2\text{O}_4$  ( $A = \text{Zn}, \text{Mg}, \text{Cd}$ ). In those compounds, since  $\text{Cr}^{3+}$  ion has the  $(3d)^3$  electron configuration, it has a spin  $S = 3/2$  and no orbital degrees of freedom. Those compounds show only one transition at  $\sim 10$  K, and we believe that this is driven by a coupling to lattice distortion as proposed in Ref. 12. A similar transition can occur at a low temperature in the vanadium spinels in principle. However, since the orbital order and subsequent magnetic transition occur at higher temperatures, this type of spin Jahn-Teller transition does not occur in the vanadium spinels in reality.

This work was supported by a Grant-in-Aid from the Ministry of Education, Science, Sports, and Culture. Parts of the numerical computations were performed on supercomputers at the Institute of the Solid State Physics, University of Tokyo, and Yukawa Institute Computer Facility, Kyoto University.

\*Present address: RIKEN (The Institute of Physical and Chemical Research), Hirosawa 2-1, Wako 351-0198, Japan.

<sup>1</sup>Y. Ueda, N. Fujiwara, and H. Yasuoka, *J. Phys. Soc. Jpn.* **66**, 778 (1997).

<sup>2</sup>S. Niziol, *Phys. Status Solidi A* **18**, K11 (1973).

<sup>3</sup>R. Liebmann, *Statistical Mechanics of Periodic Frustrated Ising Systems* (Springer, Berlin, 1986).

<sup>4</sup>J.N. Reimers, A.J. Berlinsky, and A.-C. Shi, *Phys. Rev. B* **43**, 865 (1991); J.N. Reimers, *ibid.* **45**, 7287 (1992).

<sup>5</sup>R. Moessner and J.T. Chalker, *Phys. Rev. Lett.* **80**, 2929 (1998).

<sup>6</sup>B. Canals and C. Lacroix, *Phys. Rev. B* **61**, 1149 (2000).

<sup>7</sup>A.B. Harris, J. Berlinsky, and C. Bruder, *J. Appl. Phys.* **69**, 5200 (1991).

<sup>8</sup>H. Tsunetsugu, *J. Phys. Soc. Jpn.* **70**, 640 (2001); *Phys. Rev. B* **65**, 024415 (2002).

<sup>9</sup>A. Koga and N. Kawakami, *Phys. Rev. B* **63**, 144432 (2001).

<sup>10</sup>E. Berg, E. Altman, and A. Auerbach, *Phys. Rev. Lett.* **90**, 147204 (2003).

<sup>11</sup>Y. Yamashita and K. Ueda, *Phys. Rev. Lett.* **85**, 4960 (2000).

<sup>12</sup>O. Tchernyshyov, R. Moessner, and S.L. Sondhi, *Phys. Rev. Lett.* **88**, 067203 (2002); *Phys. Rev. B* **66**, 064403 (2002).

<sup>13</sup>H. Mamiya, M. Onoda, T. Furubayashi, J. Tang, and I. Nakatani, *J. Appl. Phys.* **81**, 5289 (1997).

<sup>14</sup>N. Nishiguchi and M. Onoda, *J. Phys.: Condens. Matter* **14**, L551 (2002); M. Onoda and J. Hasegawa, *ibid.* **15**, L95 (2003).

<sup>15</sup>I. Kagomiya, K. Kohn, M. Toki, Y. Hata, and E. Kita, *J. Phys. Soc. Jpn.* **71**, 916 (2002).

<sup>16</sup>M.T. Rovers, P.P. Kyriakou, H.A. Dabkowska, G.M. Luke, M.I. Larkin, and A.T. Savici, *Phys. Rev. B* **66**, 174434 (2002).

<sup>17</sup>T. Mizokawa and A. Fujimori, *Phys. Rev. B* **54**, 5368 (1996).

<sup>18</sup>J. Matsuno, A. Fujimori, and L.F. Mattheiss, *Phys. Rev. B* **60**, 1607 (1999).

<sup>19</sup>K.I. Kugel and D.I. Khomskii, *Zh. Éksp. Teor. Fiz.* **64**, 369 (1973) [*Sov. Phys. JETP* **37**, 725 (1973)]. Our effective Hamiltonian (2) agrees with the one obtained for another  $S = 1$  system,  $\text{V}_2\text{O}_3$ , in R. Shiina, F. Mila, F.-C. Zhang, and T.M. Rice, *Phys. Rev. B* **63**, 144422 (2001), but the difference in the lattice structure will play an important role in the following discussions.

<sup>20</sup>The order by quantum fluctuations was first discussed in E.F. Shender, *Zh. Éksp. Teor. Fiz.* **83**, 326 (1982) [*Sov. Phys. JETP* **56**, 178 (1982)].